

When and why non-Hermitian eigenvalues miss eigenstates in topological physics

Lucien Jezequel,¹ Loïc Herviou,² and Jens H. Bardarson¹

¹*Department of Physics, KTH Royal Institute of Technology, Stockholm 106 91, Sweden*

²*Univ. Grenoble Alpes, CNRS, LPMMC, 38000 Grenoble, France*

Non-Hermitian systems exhibit a fundamental spectral dichotomy absent in Hermitian physics: the eigenvalue spectrum and the eigenstate spectrum can deviate significantly in the thermodynamic limit. We explain how non-Hermitian Hamiltonians can support eigenstates completely undetected by eigenvalues, with the unidirectional Hatano-Nelson model serving as both a minimal realization and universal paradigm for this phenomenon. Through exact analytical solutions, we show that this model contains not only hidden modes but multiple macroscopic hidden exceptional points that appear more generally in all systems with a non-trivial bulk winding. Our framework explains how the apparent bulk-edge correspondence failures in models like the non-Hermitian SSH chain instead reflect the systematic inability of the eigenvalue spectrum to detect certain eigenstates in systems with a skin-effect. These results establish the limitation of the eigenvalue spectrum and suggest how the eigenstate approach can lead to improved characterization of non-Hermitian topology.

Introduction—Non-Hermitian quantum mechanics has emerged as a powerful framework for describing open dissipative quantum systems, where effective Hamiltonians incorporate gain, loss [1, 2], and nonreciprocal couplings [3–5]. While such descriptions are severe approximations for weakly dissipative systems [6], recent advances have revealed that non-Hermitian physics hosts genuinely new phenomena without Hermitian counterparts. Unlike Hermitian operators, whose eigenvalues are real and whose eigenstates form a complete orthogonal basis, non-Hermitian Hamiltonians exhibit a richer spectral structure, including complex eigenvalues [7–9], exceptional points [10–16], and spectral singularities [17–21]. These features enable diverse novel phenomena, such as enhanced sensing [22–27], unidirectional invisibility [28–30], and non-Hermitian topological phases [13, 31–34].

A prominent manifestation of the anomalous non-Hermitian spectral properties is the non-Hermitian skin effect, where all eigenstates become exponentially localized at system boundaries under open boundary conditions [35–38]. Although the effect was initially discovered in one-dimensional models, it is more universal and extends to both higher dimensions [39–42] and interacting systems [43–45]. In particular, with the skin-effect there is an important difference between periodic and open boundary spectra: their band gaps may close at entirely different parameter values, and the conventional bulk-boundary correspondence fails [46–48]. Several attempts have been made to reconcile these concepts, such as the introduction of the generalized Brillouin zone [36, 49, 50], bi-orthogonal approaches [51] or proposals to focus on the stability of singular values [52–54].

In this work, we show that the failure of the bulk-edge correspondence is a direct consequence of the fact that the eigenvalue and eigenstate spectra can become different in the thermodynamic limit, where the eigenvalue spectra can miss most of the eigenstate spectra [54, 55]. This is different from Hermitian physics, where

eigenvalues and eigenstates are always linked. Using the Hatano-Nelson model as a building block, and the non-Hermitian Su-Schrieffer-Heeger (SSH) chain as an illustration, we identify not only hidden modes but hidden macroscopic exceptional points that control the spectral behavior across all skin-effect systems. These singularities explain how eigenvalue-based diagnostics can fail to detect edge states in models like the non-Hermitian SSH chain. Our findings establish the limitation of the eigenvalue spectrum and suggest how eigenstate approaches can provide better characterization of the topology.

Formal definitions.—The spectrum of a matrix or an operator H can be defined in two different ways:

Eigenvalue Spectrum: The set $\sigma_{\text{eig}}(H)$ of all eigenvalues of the operator H , which are the roots of the characteristic polynomial $\det(H - \lambda \mathbb{1})$.

Eigenstate Spectrum: The set $\sigma_{\text{states}}(H)$ of energies E for which there exists a state $|\psi\rangle$ such that $(H - E)|\psi\rangle = 0$.

These definitions coincide, $\sigma_{\text{eig}}(H) = \sigma_{\text{states}}(H)$, for finite-dimensional matrices when excluding degeneracies. They also coincide for any Hermitian operator, finite or infinite, due to the stability relation

$$\|(H - E)|\psi\rangle\| = \epsilon \implies \text{Dist}(E, \sigma_{\text{eig}}(H)) \leq \epsilon, \quad (1)$$

where $\text{Dist}(E, \sigma_{\text{eig}}(H))$ is the distance of E to the closest eigenvalue of the spectrum. This follows from the spectral theorem: in the eigenbasis $|\psi_k\rangle$ where $H|\psi_k\rangle = E_k|\psi_k\rangle$, with energies E_k , an arbitrary state $|\psi\rangle = \sum_k a_k |\psi_k\rangle$ satisfies

$$\begin{aligned} \|(H - E)|\psi\rangle\|^2 &= \sum_k |E_k - E|^2 |a_k|^2 \\ &\geq \text{Dist}(E, \sigma_{\text{eig}}(H))^2 \|\psi\|^2, \end{aligned} \quad (2)$$

and therefore $\text{Dist}(E, \sigma_{\text{eig}}(H)) \leq \epsilon$. Importantly, in the above we used the orthonormality of the eigenbasis:

$\langle \psi_k | \psi_{k'} \rangle = \delta_{k,k'}$, a property of Hermitian systems. Vice-versa, if E is an energy with $\text{Dist}(E, \sigma_{\text{eig}}(H)) = \epsilon$, then by definition there exists an eigenstate $|\psi'\rangle$ with energy E' such that $|E - E'| = \epsilon$ and

$$\|(H - E) |\psi'\rangle\| = |E' - E| = \epsilon. \quad (3)$$

In the literature, the set of energies E for which there exists a state $|\psi\rangle$ such that $\|(H - E) |\psi\rangle\| \leq \epsilon$ is called the ϵ -pseudospectrum [56], which we denote $\sigma_\epsilon(H)$.

For Hermitian operators, the constraints (2) and (3) ensure the ϵ -pseudospectrum always lies within a distance ϵ of the eigenvalue spectrum. However, this result is no longer true for non-Hermitian operators which generate important problem once we consider very large non-Hermitian systems. Indeed if we have a system of size L with Hamiltonian H_L , then in the thermodynamic limit $L \rightarrow \infty$, there is two different ways to generalize the notion of spectrum.

The eigenvalue spectrum can be defined as the limit of the roots of the characteristic polynomial, which can formally be expressed as

$$\sigma_{\text{eig}}(H_\infty) = \lim_{L \rightarrow \infty} \lim_{\epsilon \rightarrow 0} \sigma_\epsilon(H_L) \quad (4)$$

Meanwhile, the eigenstate spectrum can be defined as the set of E for which there exists states $|\psi_L\rangle$ such that $H_L |\psi_L\rangle \rightarrow 0$, which can formally be expressed as

$$\sigma_{\text{states}}(H_\infty) = \lim_{\epsilon \rightarrow 0} \lim_{L \rightarrow \infty} \sigma_\epsilon(H_L) \quad (5)$$

the fact that this two definitions no longer coincide for some non-Hermitian systems is an important result that we discuss in the rest of the paper.

The Hatano-Nelson chain, a minimal model.—The simplest model for which the eigenstate and eigenvalue spectrum differ is the leftward-hopping Hatano-Nelson model [7, 33, 34, 36, 57, 58]

$$H_L = \begin{pmatrix} 0 & 1 & & & \\ & \ddots & \ddots & & \\ & & \ddots & 1 & \\ & & & 0 & \\ & & & & \end{pmatrix}_{L \times L}, \quad (6)$$

with L sites. This model is both a physical system—a chain with hopping amplitudes—and a mathematical archetype: an order- L Jordan block exceptional point. As such, it is a simple model for understanding spectral deficiency and instabilities in non-Hermitian systems. While its eigenvalue spectrum is a single point ($\sigma_{\text{eig}}(H_L) = \{0\}$ for all L), it supports almost eigenstates for any $|E| < 1$:

$$|\psi_E\rangle = \sum_{n=0}^{L-1} E^n |n\rangle, \quad \|(H_L - E) |\psi_E\rangle\| = |E|^L \xrightarrow{L \rightarrow \infty} 0, \quad (7)$$

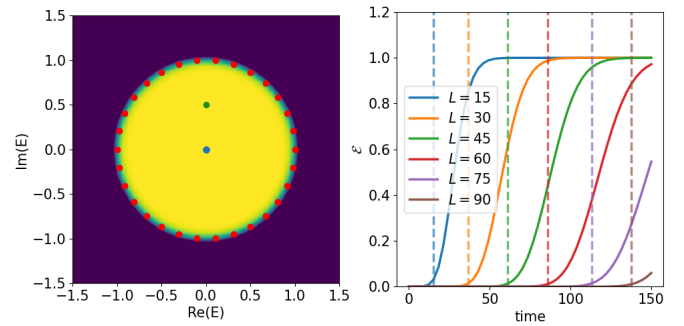


Figure 1: a) Bulk spectrum of the leftward-hopping Hatano-Nelson model (6) for $L = 30$ sites, showing periodic (red) and open boundary (blue) eigenvalue spectra. The yellow background denotes the ϵ -pseudospectrum of the open system with $\epsilon = 10^{-3}$. b) Temporal stability of the normalized state error (8) for the almost eigenstate $|\psi_E\rangle$ (7) for E at the green marker in a) showing how the state lifetime (vertical lines), until which the error remain below 1%, scales with system size.

where $|n\rangle$ are the canonical basis vectors of (6). In the thermodynamic (semi-infinite) limit $H_L \xrightarrow{L \rightarrow \infty} H_\infty$, where the order of the exceptional point goes to infinity, $\sigma_{\text{states}}(H_\infty)$ therefore contains the entire unit disk $|E| < 1$, which is much larger than the corresponding thermodynamic limit of the eigenvalue spectrum $\sigma_{\text{eig}}(H_L) \xrightarrow{L \rightarrow \infty} \{0\}$ (see Fig 1a).

In the thermodynamic limit ($L \rightarrow \infty$), as explicitly shown in Eq. (7), a sequence of states $|\psi_L\rangle$ may converge to an exact eigenstate of energy E (satisfying $\|(H_L - E) |\psi_L\rangle\| \rightarrow 0$) while the energy E may never come close to the eigenvalue spectrum $\sigma_{\text{eig}}(H_L)$ at any finite system size. This phenomenon—where the Hamiltonian has eigenstates completely undetected by its eigenvalue spectrum [52, 54, 55]—reveals an important limitation of an eigenvalue-based analysis for non-Hermitian systems. In fact, it is the root of the anomalous behavior of non-Hermitian matrices, such as their extreme sensitivity to boundary conditions close to exceptional points. In the example of Eq. (7), a perturbation of order $|E|^L$ is sufficient to make $|\psi_E\rangle$ an actual eigenvector of the finite Hamiltonian. The eigenvalue spectrum $\sigma_{\text{eig}}(H_L)$ which, without perturbation only contains $E = 0$, can therefore quickly incorporate any eigenvalue in $|E| < 1$ when allowing for even tiny perturbations. This issue typically appears in numerical algorithms where rounding errors due to the floating point precision play the role of a random perturbation [31, 56]. For instance, in the Hatano-Nelson model, we observed that numerical diagonalization with 64-bit floats produces a spectrum that qualitatively deviates from the analytical result for even moderately sized chains with $L \approx 100$. Evaluating the eigenvalue spectrum numerically is therefore inherently unstable for large systems close to an infinite order exceptional point.

The existence of almost eigenstates, like $|\psi_E\rangle$ in (7), has concrete physical implications. To quantify the stability of the almost eigenstate we define the normalized state error

$$\mathcal{E}(t) = \|e^{iHt}|\psi\rangle - e^{iEt}|\psi\rangle\|/\|e^{iEt}|\psi\rangle\|, \quad (8)$$

which quantifies the temporal stability of an almost eigenstate $|\psi\rangle$ with complex energy E under time evolution. For exact eigenstates, it remains 0 at all times. For the states $|\psi_E\rangle$ in (7), the time over which the approximation error remains small grows linearly with system size, as shown in Fig. 1b. This scaling provides a direct signature from the time evolution that these states become exact eigenstates in the thermodynamic limit.

Relationship between the eigenstate spectrum and alternative approaches to non-Hermitian spectrum.—The eigenstate spectrum can be directly connected to two alternative notions of spectrum in the literature. The first is the singular value spectrum, derived from the decomposition $H = USV^\dagger$, where U and V are unitary matrices and S is a diagonal matrix of real non-negative singular values. This spectrum is stable under perturbations and has been shown to underpin conventional topological classifications in both Hermitian and non-Hermitian models [7, 33, 52, 59]. The second is the notion of spectrum used in the mathematics literature, defined as the set of energies E for which $(H - E)$ is not invertible (i.e., $(H - E)^{-1}$ is not a bounded operator) [56]. These three approaches are in fact equivalent, meaning a complex energy E lies outside the spectrum if and only if there exists, at this energy, a spectral gap Δ which can be defined in three equivalent ways (see appendix A for a proof) associated to each approach.

Eigenstate criteria : $\forall \psi, \|(H - E)|\psi\rangle\| \geq \Delta$

Singular value criteria : $\sigma_{\min}[(H - E)^\dagger(H - E)] \geq \Delta^2$

Bounded inverse criteria : $\forall \psi, \|(H - E)^{-1}|\psi\rangle\| \leq \Delta^{-1}$

Here we only considered states acting on the right of the operator; similar definitions can be obtained for left states by replacing $H - E$ by $(H - E)^\dagger$ in the above expressions. If there is a gap for both right and left states, the singular value criteria imply that the singular value spectrum of $H - E$ has an energy gap of size Δ which justifies the name of the criteria.

The fact that the eigenstate gap can be expressed as an Hermitian gap of $(H - E)^\dagger(H - E)$ or $(H - E)(H - E)^\dagger$ imply that it is stable, in stark contrast to the different notion of eigenvalue gap around an energy E , $\Delta' = \text{Dist}(E, \sigma_{\text{eig}}(H))$ which is unstable. Moreover, the eigenstate spectrum shares a key property with Hermitian systems: in the thermodynamic limit, the spectrum under open boundary conditions contains the bulk bands of the periodic boundary spectrum (see appendix B). This is not generally true for non-Hermitian eigenvalue

spectra because of the skin effect. Therefore, the eigenstate spectrum offers much stronger theoretical stability guarantees.

The only drawback of the eigenstate spectrum is computational: determining the eigenstate spectrum requires finding the smallest singular value of $H - E$ for each energy E of interest, while the eigenvalue spectrum only requires solving one linear algebra problem. However the additional computational cost is compensated by the increased robustness of the eigenstate spectrum.

Index theorem and universality.—We now show, using topological arguments, that the Jordan block structure is in fact not limited to the model (6) but naturally emerges in any open non-Hermitian system with a non-trivial winding number. For that we start from the well-known index theorem which relates the winding number W of a bulk non-Hermitian Hamiltonian to the number of right and left edge states at the boundary [60, 61]. Taking H_{bulk} to be the periodic Hamiltonian while H has open-boundary conditions, as long as there is a (point) gap at E , the index theorem reads

$$\begin{aligned} \text{Ind}(H - E) &\equiv \dim[\ker(H - E)] - \dim[\ker(H^\dagger - \bar{E})] \\ &= W(H_{\text{bulk}} - E) \equiv \int dk \text{Tr} [(H_{\text{bulk}} - E)^{-1} \partial_k H_{\text{bulk}}(k)]. \end{aligned} \quad (9)$$

This ensure the existence of topologically protected eigenstates when $W(H_{\text{bulk}} - E) \neq 0$. In fact, such non-trivial winding has additional consequences due to the identity $W((H - E)^n) = nW(H - E)$ for any integer n . Therefore $(H - E)^n$ must have n -times more eigenstates than $H - E$. Such additional states are called generalized eigenstates as they verify $(H - E)^n|\psi\rangle = 0$ but not $(H - E)|\psi\rangle = 0$ [31]. This leads to a profound implication: a non zero winding number, $W(H - E) \neq 0$ (only possible for non-Hermitian operators), forces a proliferation of generalized eigenmodes. Specifically, if $|\psi\rangle$ is one of these new generalized eigenmodes verifying $(H - E)^n|\psi\rangle = 0$ but $(H - E)^{n-1}|\psi\rangle \neq 0$, one can check that the states $\{(H - E)^k|\psi\rangle, 0 \leq k \leq n-1\}$ form a basis on which $H - E$ acts as a Jordan block of size n like (6). This important result which holds for any integer n (as long as H^n is short-range enough compared to the lattice size). Consequently, whenever $H - E$ has non-trivial winding, the Hamiltonian must host exceptional points of macroscopic order which are typically hidden from the eigenvalue spectrum. Note that this proliferation is directly related to the so-called non-Hermitian skin effect which states that a macroscopic number of boundary states exist as long as the index of the Hamiltonian is nontrivial [37, 62].

We already discussed that the minimal model in Eq. (6) has almost eigenstates for $E \neq 0$ hidden from the eigenvalue spectrum $\sigma_{\text{eig}}(H) = \{0\}$. In fact, one can show, that it even has exceptional points for $E \neq 0$ hid-

den from $\sigma_{\text{eig}}(H)$. Indeed if we introduce the states

$$|\psi_k\rangle = \sum_n P_k(n) E^{n-k} |n\rangle \quad (10)$$

where P_k are the polynomials defined recursively by $P_0(n) = 1$ and

$$P_k(n+1) - P_k(n) = P_{k-1}(n), \quad (11)$$

then, for $|E| < 1$, one can verify that the Hamiltonian (6) acts on $|\psi_1\rangle, \dots, |\psi_m\rangle$ —up to exponentially small corrections—as a single macroscopic Jordan block of order m . This approximate Jordan-block structure holds as long as the states $|\psi_{1,\dots,m}\rangle$ have negligible amplitude at the right boundary, a condition satisfied whenever $m \ll L$. These new Jordan blocks are, by definition, exceptional points and this therefore illustrates how high-order exceptional points emerge generically in any non-Hermitian system with topological winding while often being hidden from the eigenvalue spectrum $\sigma_{\text{eig}}(H)$.

A case study: the non-Hermitian SSH model.—As a more complex example when eigenstates and exceptional points can be hidden from the eigenvalue spectrum, we study the non-Hermitian SSH model and we reinterpret its anomalous behavior. This model is a widely discussed in the non-Hermitian literature [13, 36, 49, 52, 63, 64] and its Hamiltonian is given by

$$\begin{aligned} H_{\text{nH-SSH}} = & \sum_n (t_1 - \gamma/2) |n, 2\rangle \langle n, 1| + (t_1 + \gamma/2) |n, 1\rangle \langle n, 2| \\ & + t_2 (|n+1, 1\rangle \langle n, 2| + |n, 2\rangle \langle n+1, 1|), \end{aligned} \quad (12)$$

where $|n, \alpha\rangle$ describes the orbital α at position n and all coefficients are taken positive for simplicity. The eigenvalues E_k of the bulk periodic Hamiltonian at momentum k verify:

$$E_k^2 = (t_1 + t_2 \cos k)^2 - \left(\frac{\gamma}{2} - it_2 \sin k\right)^2, \quad (13)$$

and the standard bulk gap closes for $\gamma^2 = 4(t_1 \pm t_2)^2$. With open boundary conditions, the eigenvalue phase diagram appears significantly different, with an apparent transition at $\gamma^2 = 4(t_1^2 \pm t_2^2)$ with an intermediate phase that present topological modes at zero energy (the gap closing point is obtained analytically using a non-unitary gauge transformation that absorbs the difference between left and right hopping) [36, 64].

In fact, the eigenstate spectrum of the model with open boundary conditions differs significantly from its eigenvalues (see Fig. 2a and Fig. 2b). For simplicity, we focus on the zero-energy eigenstates even if a similar analysis could be done at any energy. We place ourselves in the semi-infinite limit. Let a_n and b_n be the wavefunction amplitudes on the $|n, 1\rangle$ and $|n, 2\rangle$ sites, respectively. The modes at zero energy are known to exhibit exponential

localization at the edges under the following conditions [36, 51]:

$$\begin{aligned} \text{Left edge: } a_n &= \left(\frac{-t_1 + \gamma/2}{t_2}\right)^n, b_n = 0 \\ &\text{when } (| -t_1 + \gamma/2 | < |t_2|) \end{aligned} \quad (14)$$

$$\begin{aligned} \text{Right edge: } a_n &= 0, b_n = \left(-\frac{t_2}{t_1 + \gamma/2}\right)^{n-L} \\ &\text{when } (|t_1 + \gamma/2| < |t_2|) \end{aligned} \quad (15)$$

For finite systems, these become exponentially precise approximate modes at zero energy with errors of order $(\frac{-t_1 \pm \gamma/2}{t_2})^L$. Again we emphasize the mismatch with conventional eigenvalues, which has a vanishing eigenvalue $E \xrightarrow{L \rightarrow \infty} 0$ only when $4(t_1^2 - t_2^2) \leq \gamma^2 \leq 4(t_1^2 + t_2^2)$. This is different from the condition $|t_1 \pm \gamma/2| \leq t_2$ for the existence of an exponentially precise eigenstate (see red regions in the figures 2.c). Therefore we see that the closing of the bulk gap for values $|t_1 \pm \gamma/2| = t_2$ corresponds to the appearance or disappearance of an exponentially precise edge eigenstate but not to the appearance or disappearance of a vanishing eigenvalue. This discrepancy between the closing of the bulk gap and the moment where a vanishing eigenvalue appears for open boundary conditions has often been interpreted as bulk-edge correspondence failure, but our analysis shows that it can instead be interpreted as the eigenvalue spectrum's inability to detect eigenstates—a phenomenon already shown in the simpler model Hatano-Nelson model.

Finally, we demonstrate that the non-Hermitian SSH model, as the Hatano-Nelson model, hosts infinite families of states $|\psi_k\rangle$ forming quasi-Jordan blocks with $H|\psi_k\rangle = |\psi_{k-1}\rangle$. The coefficients $a_n^{(k)}$ and $b_n^{(k)}$ of those states take the form

$$\begin{aligned} a_n^{(k)} &= P_k(n) r^n & b_n &= 0 & \text{if } n \text{ odd} \\ a_n^{(k)} &= 0 & b_n &= P_k(n) r^n & \text{if } n \text{ even} \end{aligned} \quad (16)$$

with $r = \frac{-t_1 + \gamma/2}{t_2}$ and $r' = \frac{-t_2}{t_1 + \gamma/2}$ and $P_k(n)$ are polynomials generated recursively with $P_0(n) = 1$ and the recursive relation

$$\begin{aligned} P_{k+1}(n+1) - r'/r P_{k+1}(n) &= P_k(n) & \text{if } k \text{ odd} \\ P_{k+1}(n+1) - P_{k+1}(n) &= P_k(n) & \text{if } k \text{ even} \end{aligned} \quad (17)$$

For finite systems, the block survives up to exponential corrections as long as the modes have small amplitudes on the right edge which is true as long as $n \ll L$. This example illustrates again the general proximity of non-Hermitian Hamiltonians to macroscopic-order Jordan blocks, the fundamental reason behind their instability, despite an apparently well-defined eigenvalue spectrum.

Conclusions and discussions.—In this work, we have shown that some of the discrepancies arising in the study

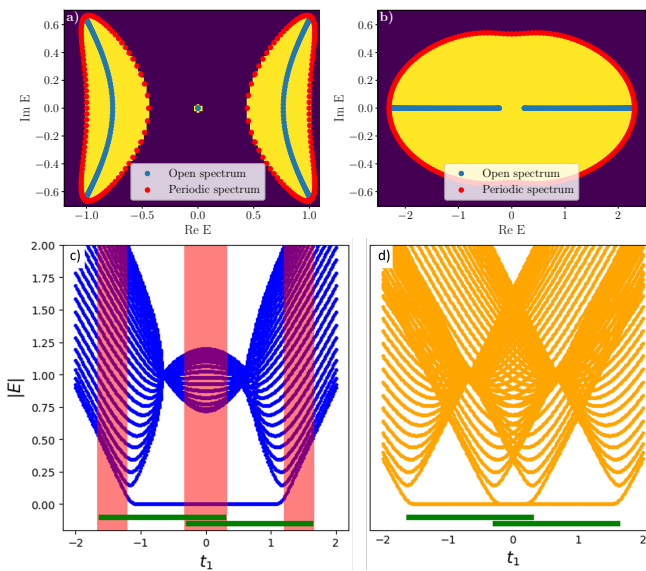


Figure 2: a) Spectrum of the non-Hermitian SSH model defined in Eq. (12) for $(t_1, t_2, \gamma) = (0.2, 1, 4/3)$ and $L = 100$. The dots correspond to the eigenvalue spectrum for periodic and open boundary conditions, while the yellow background is the eigenstate spectrum of the open system. It is the full area enclosed by the periodic spectrum. b) Similar spectrum for $(t_1, t_2, \gamma) = (1.4, 1, 4/3)$. Note that now eigenstates with zero energy are present despite the absence of topological modes in the eigenvalue spectrum. Plot of c) eigenvalue spectrum and d) singular value spectrum for $(t_2, \gamma) = (1, 4/3)$ and $L = 20$ sites with open boundary conditions, reproducing the configuration of [36]. Parameters for which topological edge modes at zero energy exist are denoted in green. The eigenvalue spectrum is deficient in the red regions with either a gap while there is one mode at zero energy ($1.2 \lesssim |t_1| \leq 5/3$) or a single zero eigenvalue where there is two modes at zero energy ($|t_1| \leq 1/3$). Singular value has however no problem detecting those modes at zero energy.

of non-Hermitian systems are due to the use of eigenvalue spectrum instead of eigenstate spectrum. The eigenstate spectrum is generally stable and well-defined, and reproduce well-known results due to its connection to singular value analysis. At the same time, it gives a much-needed and clear interpretation of the instabilities inherent to non-Hermitian systems. The instabilities are simply a consequence of the eigenvalue spectrum missing (nearly all) eigenstates of operators in the thermodynamic limit. In this paper we showed that the instabilities can also be understood as a consequence of the proximity of hidden macroscopic Jordan blocks that proliferate in the thermodynamic limit. Contrary to what their name may suggests, this shows that *exceptional* points are not always rare and can appear in a dense part of the spectrum and of the parameter space. This lead to the presence of hidden eigenstates which have physical consequences. During time evolution, they behave as eigenstates for a macroscopic duration, before the finite-size effects kick

in.

Our single-particle framework extends directly to many-body bosonic systems in the limit of weak interactions. Fermionic systems, on the other hand, exhibit rich Pauli-driven localization transitions invisible to eigenvalue diagnostics [45, 65–67]. The relations between these transitions and eigenstate transitions appear to be an interesting direction for future research. In conclusion, the universal presence of spectral singularities demands a paradigm shift: state-centric analysis is indispensable for non-Hermitian topology, many-body physics, and beyond.

Acknowledgment We thank Emil Bergholtz and Fan Yang for insightful discussions. L.J and J.B acknowledge financial support by the Swedish Research Council (VR) through Grant No. 2020-00214, and the European Research Council (ERC) under the European Union’s Horizon 2020 research and innovation program (Grant Agreement No. 101001902). L.H. acknowledges financial support by the CNRS through the Tremplin funding.

- [1] L. Feng, R. El-Ganainy, and L. Ge, *Nature Photonics* **11**, 752 (2017).
- [2] S. Liu, S. Ma, C. Yang, L. Zhang, W. Gao, Y. J. Xiang, T. J. Cui, and S. Zhang, *Phys. Rev. Appl.* **13**, 014047 (2020).
- [3] H.-K. Lau and A. A. Clerk, *Nature Communications* **9**, 4320 (2018).
- [4] M. Fruchart, R. Hanai, P. B. Littlewood, and V. Vitelli, *Nature* **592**, 363–369 (2021).
- [5] M. Reisenbauer, H. Rudolph, L. Egyed, K. Hornberger, A. V. Zasedatelev, M. Abuzarli, B. A. Stickler, and U. Delić, *Nature Physics* **20**, 1629 (2024).
- [6] F. Roccati, G. M. Palma, F. Ciccarello, and F. Bagarello, *Open Systems & Information Dynamics* **29**, 2250004 (2022).
- [7] K. Kawabata, K. Shiozaki, M. Ueda, and M. Sato, *Phys. Rev. X* **9**, 041015 (2019).
- [8] K. Wang, A. Dutt, C. C. Wojcik, and S. Fan, *Nature* **598**, 59 (2021).
- [9] F. Schindler, K. Gu, B. Lian, and K. Kawabata, *PRX Quantum* **4**, 030315 (2023).
- [10] W. D. Heiss, *Journal of Physics A: Mathematical and General* **37**, 2455–2464 (2004).
- [11] F. Minganti, A. Miranowicz, R. W. Chhajlany, and F. Nori, *Phys. Rev. A* **100**, 062131 (2019).
- [12] M.-A. Miri and A. Alù, *Science* **363**, eaar7709 (2019).
- [13] E. J. Bergholtz, J. C. Budich, and F. K. Kunst, *Rev. Mod. Phys.* **93**, 015005 (2021).
- [14] K. Wang, L. Xiao, J. C. Budich, W. Yi, and P. Xue, *Phys. Rev. Lett.* **127**, 026404 (2021).
- [15] Q. Liao, C. Leblanc, J. Ren, F. Li, Y. Li, D. Solnyshkov, G. Malpuech, J. Yao, and H. Fu, *Phys. Rev. Lett.* **127**, 107402 (2021).
- [16] P. Delplace, T. Yoshida, and Y. Hatsugai, *Phys. Rev. Lett.* **127**, 186602 (2021).
- [17] Q. Zhong, M. Khajavikhan, D. N. Christodoulides, and R. El-Ganainy, *Nature Communications* **9**, 4808 (2018).

[18] J.-W. Ryu, J.-H. Han, and C.-H. Yi, *Phys. Rev. A* **106**, 012218 (2022).

[19] L. Jezequel and P. Delplace, *Phys. Rev. Lett.* **130**, 066601 (2023).

[20] A. Leclerc, L. Jezequel, N. Perez, A. Bhandare, G. Laibe, and P. Delplace, *Phys. Rev. Res.* **6**, L012055 (2024).

[21] F. Zhang, N. S. Solodovchenko, H. Fan, M. F. Limonov, M. Song, Y. S. Kivshar, and A. A. Bogdanov, *Science Advances* **11**, eadr9183 (2025).

[22] J. Wiersig, *Phys. Rev. Lett.* **112**, 203901 (2014).

[23] W. Chen, S. Kaya Özdemir, G. Zhao, J. Wiersig, and L. Yang, *Nature* **548**, 192 (2017).

[24] H. Hodaei, A. U. Hassan, S. Wittek, H. Garcia-Gracia, R. El-Ganainy, D. N. Christodoulides, and M. Khajavikhan, *Nature* **548**, 187 (2017).

[25] C. Chen, L. Jin, and R.-B. Liu, *New Journal of Physics* **21**, 083002 (2019).

[26] R. Kononchuk, J. Cai, F. Ellis, R. Thevamaran, and T. Kottos, *Nature* **607**, 697 (2022).

[27] J. Wiersig, *Nature Communications* **11**, 2454 (2020).

[28] S. Longhi, *Optics Letters* **40**, 5694 (2015).

[29] A. Brandstötter, K. G. Makris, and S. Rotter, *Phys. Rev. B* **99**, 115402 (2019).

[30] S. Longhi and E. Pinotti, *Phys. Rev. B* **106**, 094205 (2022).

[31] Y. Ashida, Z. Gong, and M. Ueda, *Advances in Physics* **69**, 249–435 (2020).

[32] S. Yao, F. Song, and Z. Wang, *Phys. Rev. Lett.* **121**, 136802 (2018).

[33] Z. Gong, Y. Ashida, K. Kawabata, K. Takasan, S. Higashikawa, and M. Ueda, *Phys. Rev. X* **8**, 031079 (2018).

[34] H. Shen, B. Zhen, and L. Fu, *Phys. Rev. Lett.* **120**, 146402 (2018).

[35] H. Zhou, C. Peng, Y. Yoon, C. W. Hsu, K. A. Nelson, L. Fu, J. D. Joannopoulos, M. Soljačić, and B. Zhen, *Science* **359**, 1009–1012 (2018).

[36] S. Yao and Z. Wang, *Phys. Rev. Lett.* **121**, 086803 (2018).

[37] N. Okuma, K. Kawabata, K. Shiozaki, and M. Sato, *Phys. Rev. Lett.* **124**, 086801 (2020).

[38] X. Zhang, T. Zhang, M.-H. Lu, and Y.-F. Chen, *Advances in Physics: X* **7**, 2109431 (2022).

[39] K. Zhang, Z. Yang, and C. Fang, *Nature Communications* **13**, 2496 (2022).

[40] H.-Y. Wang, F. Song, and Z. Wang, *Phys. Rev. X* **14**, 021011 (2024).

[41] H. Hu, *Science Bulletin* **70**, 51 (2025).

[42] F. Yang and E. J. Bergholtz, *Phys. Rev. Res.* **7**, 023233 (2025).

[43] R. Shen and C. H. Lee, *Communications Physics* **5**, 238 (2022).

[44] F. Yang, Q.-D. Jiang, and E. J. Bergholtz, *Phys. Rev. Res.* **4**, 023160 (2022).

[45] F. Alsallom, L. Herviou, O. V. Yazyev, and M. Brzezinska, *Phys. Rev. Res.* **4**, 033122 (2022).

[46] T. E. Lee, *Phys. Rev. Lett.* **116**, 133903 (2016).

[47] Y. Xiong, *Journal of Physics Communications* **2**, 035043 (2018).

[48] H. Spring, V. Könye, A. R. Akhmerov, and I. C. Fulga, *SciPost Phys.* **17**, 153 (2024).

[49] F. Song, S. Yao, and Z. Wang, *Phys. Rev. Lett.* **123**, 246801 (2019).

[50] Z. Yang, K. Zhang, C. Fang, and J. Hu, *Phys. Rev. Lett.* **125**, 226402 (2020).

[51] F. K. Kunst, E. Edvardsson, J. C. Budich, and E. J. Bergholtz, *Phys. Rev. Lett.* **121**, 026808 (2018).

[52] L. Herviou, J. H. Bardarson, and N. Regnault, *Phys. Rev. A* **99**, 052118 (2019).

[53] D. Porras and S. Fernández-Lorenzo, *Phys. Rev. Lett.* **122**, 143901 (2019).

[54] K. Monkman and J. Sirker, *Phys. Rev. Lett.* **134**, 056601 (2025).

[55] Y. Mardani, R. A. Pimenta, and J. Sirker, *arXiv:2410.01542*.

[56] L. N. Trefethen and M. Embree, *Spectra and pseudospectra: the behavior of nonnormal matrices and operators* (Princeton university press, 2020).

[57] N. Hatano and D. R. Nelson, *Phys. Rev. Lett.* **77**, 570 (1996).

[58] N. Hatano and D. R. Nelson, *Phys. Rev. B* **58**, 8384 (1998).

[59] C.-H. Liu, H. Jiang, and S. Chen, *Phys. Rev. B* **99**, 125103 (2019).

[60] C. L. Kane and T. C. Lubensky, *Nature Physics* **10**, 39–45 (2013).

[61] L. Jezequel and P. Delplace, *SciPost Phys.* **17**, 060 (2024).

[62] K. Zhang, Z. Yang, and C. Fang, *Phys. Rev. Lett.* **125**, 126402 (2020).

[63] C. Yin, H. Jiang, L. Li, R. Lü, and S. Chen, *Phys. Rev. A* **97**, 052115 (2018).

[64] R. Lin, T. Tai, L. Li, and C. H. Lee, *Frontiers of Physics* **18**, 53605 (2023).

[65] M. Zheng, Y. Qiao, Y. Wang, J. Cao, and S. Chen, *Phys. Rev. Lett.* **132**, 086502 (2024).

[66] S. Hamanaka and K. Kawabata, *Phys. Rev. B* **111**, 035144 (2025).

[67] P. Zhong, W. Pan, H. Lin, X. Wang, and S. Hu, *Phys. Rev. Lett.* **135**, 106502 (2025).

Appendix A: Equivalence between the different notions of spectrum

In this appendix, we demonstrate that the eigenstate approach, the singular value spectrum, and the bounded inverse spectrum discussed in the main text provide equivalent characterizations of a spectral gap. We focus exclusively on the *right gap* case; the proof for the left gap follows identically upon taking $H' = H^\dagger$.

Let $A = H - E$. For $\Delta > 0$, we want to show that the following three criteria are equivalent:

$$\text{Pseudospectrum criteria: } \forall |\psi\rangle, \|A|\psi\rangle\| \geq \Delta \|\psi\|. \quad (\text{A1})$$

$$\text{Singular value criteria: } \sigma_{\min}(A^\dagger A) \geq \Delta^2. \quad (\text{A2})$$

$$\text{Bounded inverse criteria: } \forall |\phi\rangle, \|A^{-1}|\phi\rangle\| \leq \Delta^{-1} \|\phi\|. \quad (\text{A3})$$

Equivalence between (A1) and (A2): Squaring the inequality in (A1) gives

$$\|A\psi\|^2 = \langle\psi|A^\dagger A|\psi\rangle \geq \Delta^2 \langle\psi|\psi\rangle \quad \forall|\psi\rangle. \quad (\text{A4})$$

This inequality means that the operator $A^\dagger A$ has all eigenvalues greater than or equal to Δ^2 , which in turn implies that its smallest eigenvalue satisfies $\sigma_{\min}(A^\dagger A) \geq \Delta^2$. Since the smallest singular value squared of A equals the smallest eigenvalue of $A^\dagger A$, that is, $\sigma_{\min}(A^\dagger A)$, we recover (A2). Conversely if $\sigma_{\min}(A^\dagger A) \geq \Delta^2$, we have the inequality (A4) and therefore (A1).

Equivalence between (A1) and (A3): Suppose (A1) holds. For any state $|\phi\rangle$, define $|\psi\rangle = A^{-1}|\phi\rangle$. Substituting into (A1) yields

$$\|\phi\| = \|A\psi\| \geq \Delta\|\psi\| = \Delta\|A^{-1}\phi\|, \quad (\text{A5})$$

which implies $\|A^{-1}\phi\| \leq \Delta^{-1}\|\phi\|$, and therefore (B3). Conversely, if (A3) holds, set $|\phi\rangle = A|\psi\rangle$. Then (A3) gives $\|\psi\| \leq \Delta^{-1}\|A\psi\|$, which is exactly (A1).

Since (A1) is equivalent to both (A2) and (A3), all three criteria are mathematically equivalent.

Appendix B: Eigenstate spectrum and open boundary conditions

In this appendix we show that for any local non-Hermitian Hamiltonian, the eigenstate spectrum share the property of the Hermitian spectrum that the open boundary condition spectrum includes, in the thermodynamic limit, the bulk bands of the periodic boundary condition spectrum. For periodic Hamiltonian H_{PBC} we can make the distinction between the unit cell number n and internal degrees of freedom α of the unit cell on which the Hamiltonian is periodic.

The eigenstate of the periodic Hamiltonian will then take the form of Bloch state with

$$|\psi\rangle = \sum_x e^{ikx} c_\alpha |x, \alpha\rangle \quad (\text{B1})$$

with quasimomentum k and energy E .

If we then consider the same Hamiltonian but with open-boundary condition H_{OBC} , we can construct from this Bloch state, a state $|\psi'\rangle$ which is an eigenstate of H_{OBC} up to an error which vanishes in the large length limit. This state is the following

$$|\psi'\rangle = \sum_{x, \alpha} e^{ikx} g(x/L) c_\alpha |x, \alpha\rangle = g(\hat{x}/L) |\psi\rangle \quad (\text{B2})$$

where $g(x/L)$ is a smooth envelope function vanishing at the boundaries. The slow variation of $g(x/L)$ on the scale of the lattice constant ensures that $\|[H_{\text{OBC}}, g(\hat{x}/L)]\| = O(1/L)$. This, together with the vanishing of $g(x/L)$ at the boundaries ensure that the amplitude of $|\psi'\rangle$ is negligible near the boundary which suppresses boundary-related errors by a factor $O(1/L)$, implies that the resulting state has a small energy variance:

$$\begin{aligned} \|(H_{\text{OBC}} - E)g(\hat{x}/L)|\psi'\rangle\| &= \|(H_{\text{PBC}} - E)g(\hat{x}/L)|\psi\rangle\| + O(1/L) \\ &= \|g(\hat{x}/L)(H_{\text{PBC}} - E)|\psi\rangle\| + \|[H_{\text{PBC}}, g(\hat{x}/L)]|\psi\rangle\| + O(1/L) = O(1/L) \end{aligned} \quad (\text{B3})$$

where we used that $(H_{\text{PBC}} - E)|\psi\rangle = 0$ as $|\psi\rangle$ is an eigenstate of the periodic Hamiltonian. This proves that all periodic bulk eigenstates have open-boundary counterparts in the eigenstate spectrum for large enough systems.